

Raman scattering studies of the impurity-induced ferroelectric phase transition in $\text{KTaO}_3\text{:Nb}$

R. L. Prater and L. L. Chase

Physics Department, Indiana University, Bloomington, Indiana 47405

L. A. Boatner

Solid State Division, Oak Ridge National Laboratory, Oak Ridge, Tennessee 37830

(Received 2 June 1980)

Raman scattering and optical-depolarization measurements have been employed in investigations of the ferroelectric phase transition in $\text{KTa}_{1-x}\text{Nb}_x\text{O}_3$ in the limit $x \leq 0.05$. The critical niobium concentration for which $T_c \approx 0$ K was found to be $x_c = 0.008$, in agreement with previous acoustic resonance results. Electric-field-induced Raman scattering and disorder-induced Raman scattering were used to study the zone-center TO frequency as a function of x and temperature. At a given temperature, the TO frequency decreases with increasing x , and no new low-frequency vibrational features due to the Nb are observed. The Raman spectra as a function of temperature are indicative of a soft-mode-dominated displacive transition to a rhombohedral ferroelectric phase. The soft-mode frequencies in both phases, however, remain finite ($\sim 10 \text{ cm}^{-1}$) in the immediate vicinity of T_c . Disorder-induced scattering features in the paraelectric phase in all of the samples (including pure KTaO_3) are attributed to first-order scattering from the coupled TO and TA branches. The TA peak has previously been associated with a resonance mode of lithium impurities. The observed TA scattering was modeled using parameters obtained previously from neutron scattering investigations, and good agreement was found for the frequency of this feature as a function of the soft-mode energy. The presence of Nb has no effect on the intensity of any of the disorder-induced features, and the exact source of the disorder is currently undetermined.

I. INTRODUCTION

Potassium tantalate is a cubic perovskite-structure material that exhibits the characteristics of a ferroelectric whose transition temperature is near absolute zero. In the purest KTaO_3 samples investigated no transition to a ferroelectric phase has been observed at temperatures as low as 1.6 K. Potassium tantalate and strontium titanate are currently the only two known substances which exhibit this type of behavior, and the term "incipient ferroelectric" has been applied to these special materials. For both KTaO_3 and SrTiO_3 , deviations of the behavior of the dielectric constant from a Curie-law dependence have been attributed to the presence of a paraelectric phase that is "quantum stabilized." This means that a transition to the distorted ferroelectric structure would lead to an increase in the quantum-mechanical zero-point energy of the lattice which more than compensates for the decreased classical potential energy of the ferroelectric phase.

The presence of even small concentrations of certain impurities induces a ferroelectric phase in KTaO_3 at low temperatures, and this effect proved to be a hindrance to an accurate delineation of the unique properties of pure KTaO_3 in the earliest studies of

this substance. This effect is of interest in itself, and affords the opportunity for investigations that can lead to answers to a number of questions of current interest. These questions include: First, what are the mechanisms by which low impurity levels can drastically modify the bulk properties of a crystal? Second, can different impurities induce ferroelectricity by means of totally different mechanisms? Finally, what are the key features characterizing a given impurity and how do these features influence the ferroelectric phase induced by the impurity? Additionally, studies of controlled impurity levels can provide information on the nature of defect-induced central peaks and the manner in which central peaks reflect either the coupling of a defect to the order parameter or other perturbations of the lattice.

The existing body of work on KTaO_3 , $\text{KTa}_{1-x}\text{Nb}_x\text{O}_3$, and related materials provides a basis for the present studies of impurity effects and the associated phase transitions in these systems. The available data for KTaO_3 include determinations of the dielectric response over a wide range of frequencies,¹⁻³ and measurements of the dielectric constant as a function of temperature and pressure.^{4,5} Dielectric response measurements have been correlated with thermal expansion and compressibility data ob-

tained from x-ray-diffraction measurements,⁶ and the effects of uniaxial stress on the dielectric response of KTaO_3 at low frequencies have also been investigated.^{7,8} Most recently, the polarization moment and elastic compliance were measured by Höchli and Boatner¹ by means of ultrasonic flexure-resonance spectroscopy.

Other investigations that are pertinent to the present work include the dielectric constant measurements for $\text{KTa}_{1-x}\text{Nb}_x\text{O}_3$ (KTN) which were made as early as 1959 by Triebwasser,⁹ and the more recent determinations of the dielectric constant, spontaneous polarization, and elastic compliance of KTN made by Höchli *et al.*^{10,11} Trivalent iron has been used as a probe ion in recent EPR studies of the lattice properties of KTN,¹² and the lattice dynamics of KTN in each of its phases have been extensively studied using neutron scattering techniques.¹³⁻¹⁵ Neutron scattering measurements were also made for pure KTaO_3 by Shirane *et al.*¹⁶ and Axe *et al.*,¹⁷ and, most recently, Comés and Shirane¹⁸ have considered the anisotropy of the phonon dispersion in pure KTaO_3 .

The earliest investigations of KTaO_3 involving the use of optical techniques consisted of measurements of the infrared reflectivity at various temperatures^{19,20} and the Raman scattering studies of Nilsen and Skinner²¹ and Perry *et al.*²² More recently Fleury and Worlock^{23,24} have used Raman scattering techniques to measure the soft-mode position in pure KTaO_3 by applying an ac electric field and observing the resulting field-induced scattering component. Yacoby and Linz²⁵ have measured the Raman spectra of both pure KTaO_3 and samples containing either Nb or Li impurities. The first study of KTN using Raman scattering was made by Manliet and Fan.²⁶ Changes in the Raman spectra due to applied pressure have been studied by Yacoby *et al.*,²⁷ and changes due to uniaxial stress were investigated by Uwe and Saku-do.²⁸ Yacoby²⁹ recently studied the Raman spectrum of KTN in a sample containing 6 at. % Nb and concluded that the individual distorted Nb centers produce fluctuations whose amplitudes decrease for $T > T_c$.

In the present work, Raman scattering techniques have been used to investigate the characteristics of impurity-induced phase transitions in potassium tantalate-niobate crystals with Nb concentrations in the range from 0.25 to 5.0 at. %. By employing samples with varying compositions within this range, it was possible to test whether or not some of the features reported in the previously noted studies were associated directly with the presence of Nb or with the induced phase transitions.

Since every atom in the unit cell of the perovskite structure occupies a site with inversion symmetry, one-phonon Raman scattering is forbidden in the paraelectric phase. Therefore, any inelastic light

scattering is due either to two-phonon processes, impurity-induced scattering, or scattering induced by any disorder in the crystal which breaks the wave-vector selection rules. To determine the effects of Nb impurities on the lowest TO branch at $k = 0$, electric-field-induced Raman scattering was measured in samples with different Nb concentrations. Measurements were also made of the birefringence and optical depolarization of KTN single crystals as a function of temperature, in order to obtain an independent determination of the transition temperature of each sample.

II. EXPERIMENTAL METHODS

The Raman scattering spectrometer employed in the present work consisted of a coherent radiation model 52 argon-ion laser as the excitation source, a Spex model 1400 double monochromator for dispersion, and a cooled I.T.T. FW 130 phototube for detection. The system was arranged in the conventional 90° scattering geometry. A PDP 11/03 microcomputer was used for digital collection of the data, which were transmitted to a PDP 11/34 minicomputer and stored on a floppy disk.

KTN and KTaO_3 single-crystal samples were mounted in a copper enclosure provided with entrance and exit holes for the laser light and a slot for transmission of the scattered light image. A thin layer of silicone vacuum grease was used to enhance the thermal contact between the sample and the copper enclosure. The sample assembly was placed in a Janis stainless steel liquid-helium Dewar, in which the sample temperature could be controlled by varying the exchange gas pressure and by heating the copper enclosure with an attached resistance element. Sample temperatures were measured using an Fe: Au vs Chromel thermocouple mounted near the crystal in a small hole in the copper enclosure. A conservative estimate of the accuracy of the temperature measurement is ± 0.5 K over the range from 4.2 K to room temperature. The samples employed in studies of electric-field-induced scattering were prepared by depositing a gold film on two major opposing faces of the crystal. The sample was then mounted in the holder by means of a Teflon strip with the high voltage lead inserted between this strip and one of the gold-coated faces. In this arrangement, the opposite gold-coated face of the crystal was held in close contact with the copper enclosure to form both the ground connection and a good heat sink for the sample. Possible charging effects due to photocurrents were minimized by employing a circuit which allowed the application of a large-amplitude sinusoidal voltage with no dc component.

Phase-sensitive detection at twice the frequency of the applied voltage was used to enhance detection of

the electric-field-induced component of the scattered light. By monitoring the input to the lock-in amplifier, the total scattered Raman signal could be recorded simultaneously with the electric-field-induced component.

Measurements of the birefringence or depolarization were made with a low-power defocused beam in order to minimize local heating effects. The incoming beam was polarized along a cube axis, and measurements were made of the intensities of the components of the exiting beam which were polarized parallel (I_{\parallel}) and perpendicular (I_{\perp}) to the incoming beam polarization. The depolarization ratio, defined as

$$R = \frac{I_{\parallel} - I_{\perp}}{I_{\parallel} + I_{\perp}},$$

was then plotted as a function of temperature.

The single crystals of KTN used in these investigations were grown in a Pt crucible from mixtures of K_2CO_3 , Ta_2O_5 , and varying amounts of Nb_2O_5 . An excess of K_2CO_3 and minute traces of CuO or TiO_2 were added to facilitate the growth of optical quality single crystals. The data are reported using concentrations calculated from the molar ratio of Nb_2O_5 to Ta_2O_5 in the initial mixture. Details of the crystal growth process can be found elsewhere.³⁰ Observation of the cut and polished single crystals between crossed polarizers indicates a considerable variation in internal strain distribution from one sample to another.

III. EXPERIMENTAL RESULTS AND ANALYSIS

A. Low-frequency features in the Raman spectrum of pure $KTaO_3$

The Raman scattering observed for pure $KTaO_3$ at $T = 4.2$ K is shown in Fig. 1 on a scale that emphasizes the low-frequency features. The sharp peak at 90 cm^{-1} was identified previously²¹ as two-phonon scattering that arises from a peak in the density of states of the transverse-acoustic branch at the zone boundary. The inset in Fig. 1 shows that this peak softens when the temperature is lowered from 77 to 4.2 K. The shoulder evident on the low-frequency side of the 2TA peak in Fig. 1 is most pronounced at lower temperatures; it becomes less well defined and moves up in frequency with increasing temperature. Due to its broad nature and possible association with the 2TA peak, this shoulder has always been identified as arising from two-phonon scattering. As indicated by the arrows in Fig. 1, however, the position of the onset of the shoulder correlates remarkably well over a wide temperature range with the energy of the lowest transverse optic mode at the zone center as determined from neutron scattering. This correlation, which is more clearly demonstrated by

the electric-field-induced scattering results discussed in Sec. III C, leads to the conclusion that the shoulder is due to first-order scattering from the soft TO branch. Such scattering could be induced by intrinsic disorder or by remanent impurities which can be present in even the purest available crystals. This possibility will be discussed further in Sec. IV. The small peak which is shown just below the shoulder in Fig. 1(a) represents the third major feature in the low-energy spectrum. This peak increases in energy with increasing temperature, and remains below the onset of the shoulder. The peak broadens and loses intensity as the temperature increases and cannot be observed above 77 K. The intensity of this line was enhanced by the addition of a few tenths of an atomic percent of Li as discussed elsewhere.³¹ A significant aspect of all of the low-frequency features observed for pure $KTaO_3$ is that they are strongly polarized along the direction of the incident laser light polarization.

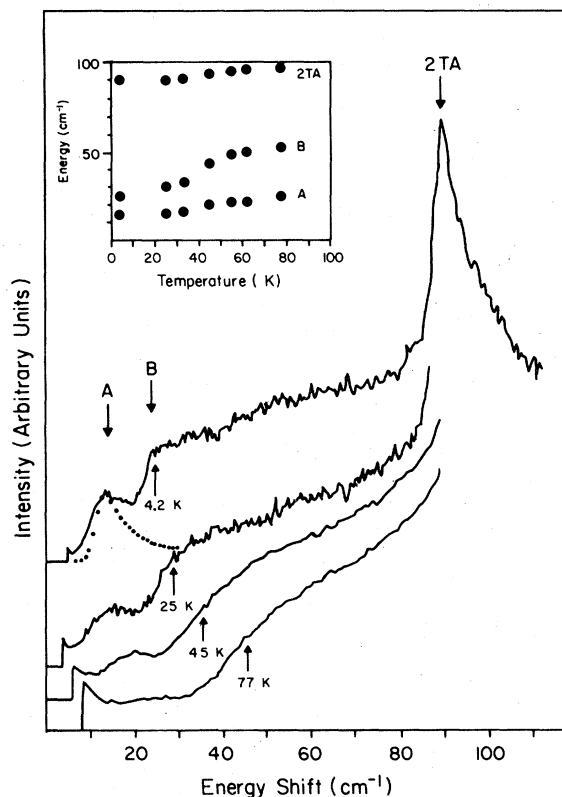


FIG. 1. Raman scattering spectra of pure $KTaO_3$ at various temperatures. The arrow for each temperature indicates the energy of the zone-center TO_1 phonon as determined from neutron scattering experiments (Ref. 16). The dotted curve indicates the shape of the TA peak at 4.2 K derived from the theory described in Sec. IV. Inset: The energy of the three low-frequency features vs temperature.

B. Raman spectra of $\text{KTaO}_3\text{:Nb}$

The major change in the properties of KTaO_3 resulting from the introduction of Nb impurities is the appearance of a transition to a low-temperature ferroelectric phase. The critical temperature of this transition can be controlled by varying the Nb content, and changes in the Raman spectra are to be correlated with the transition temperature. Two methods were used in order to determine the transition temperatures for crystals with different Nb concentrations. One method was based on the observation of changes in the Raman spectra that occur as the lattice symmetry changes. Such changes are illustrated in Fig. 2 for a $\text{KTa}_{0.98}\text{Nb}_{0.02}\text{O}_3$ sample. As the temperature is lowered below T_c (about 28 K in this sample), an intense peak appears. This peak, which can be seen in Fig. 2 near 20 cm^{-1} at 16.5 K, increases in intensity and moves up in energy as the temperature is decreased below T_c . In the samples containing more than 3 at. % Nb, the peak splits into two peaks when the temperature is lowered to 4.2 K. These peaks correspond to the lowest transverse optic modes, which are Raman active in the rhombohedral-symmetry ferroelectric phase. In a true soft-mode phase transition, the Raman-active soft-mode energy should approach zero as the temperature approaches T_c from below. In all of our samples containing Nb impurities, this mode was resolved with energies as low as 10 cm^{-1} near T_c , but the square of the energy as a function of temperature cannot be extrapolated linearly to zero at T_c as would be expected from the results of mean-field theory. In the cubic paraelectric phase, first-order Raman scattering is symmetry forbidden and these features disappear as expected.

It should be noted that in all of the present measurements both the Raman and the depolarization results are consistent with a ferroelectric phase that has rhombohedral symmetry. This symmetry would be expected in KTN with a Nb concentration below the multicritical concentration, as discussed by Boatner *et al.*³² At the multicritical concentration, the two phase transitions (i.e., from cubic to orthorhombic and from orthorhombic to rhombohedral symmetry) become a single transition from cubic symmetry directly to the rhombohedral phase. All of the samples have Nb concentrations below the multicritical point of the phase diagram, and we see no evidence which would suggest that the ferroelectric phase has anything but rhombohedral symmetry.

An alternate method for determining the transition temperature in these samples is to measure the depolarization of light as it passes through the crystal. In the cubic phase, the optical properties are isotropic and there is no depolarization. In the ferroelectric phase, however, the optical constants are anisotropic; for a multidomain sample, this anisotropy will pro-

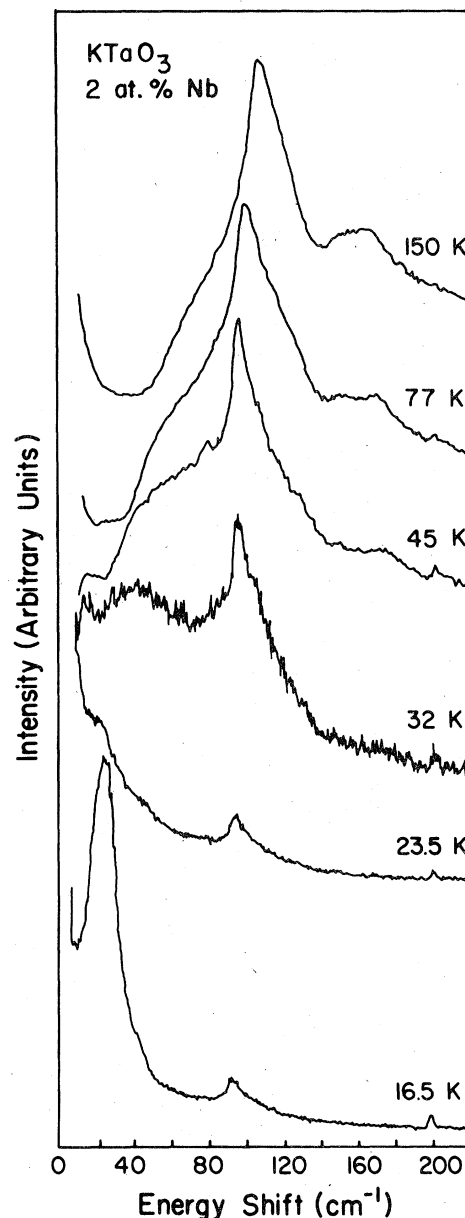


FIG. 2. Raman spectra at various temperatures for a KTaO_3 sample containing 2 at. % Nb. The gain in the 23.5- and 16.5-K traces is reduced by approximately a factor of 5.

duce a depolarization of the transmitted light due to multiple alterations of the polarization by the various domains. This behavior is apparent from the data presented in Fig. 3. For the 5 and 3.2 at. % Nb samples, the depolarization is complete and occurs in a relatively narrow temperature interval. The transition is substantially sharper in the 3.2 at. % sample ($\Delta T \sim 1\text{ K}$) than in the 5 at. % sample ($\Delta T > 5\text{ K}$). In the 5, 2, and 0.8 at. % samples, the small oscillations above and below the transition are associ-

ated with the presence of a relatively small number of domains across the sample thickness of 2 to 4 mm. In the sample with an 0.8 at. % Nb concentration (the critical concentration for ferroelectricity at 0 K), the depolarization is not complete even at 4 K. This suggests either that there is a small anisotropy in each domain or that only a small number of regions of the sample are ferroelectric. These conclusions are reinforced by the fact that the depolarization data below the phase transition in the 0.8 and 2 at. % are not exactly reproducible. The oscillatory depolarization effects are observed at reproducible temperatures in each sample, but the exact values of the depolarization ratio are not duplicated from one measurement to another. In summary, these depolarization measurements imply that domains exist which are large compared to an optical wavelength and that there are substantial differences in the transition temperature in different regions of some samples.

An indication of the modifications to the two low-frequency features of the pure KTaO_3 spectrum resulting from the addition of Nb impurities is illustrated in Fig. 2. The shoulder is observed to soften considerably as the phase transition is approached from high temperature, and the peak remains just below the shoulder as long as it can be distinguished. The position of the peak as a function of temperature for several Nb concentrations is plotted in Fig. 4, and the temperature of the phase transition onset is noted for each case. It can be seen that there is a noticeable softening of the peak (and shoulder) energies from their value in pure KTaO_3 when the sample incorporates only 0.25 at. % Nb, which is less than half the concentration required to induce a ferroelectric phase transition.

The most important characteristic of the low-frequency features in KTN is that there is no intensity change as the Nb concentration is increased to over 5 at. %. This indicates that the low-energy peak is neither a resonance mode nor any other impurity effect induced by the presence of the Nb. Also, if the shoulder is a manifestation of impurity-induced

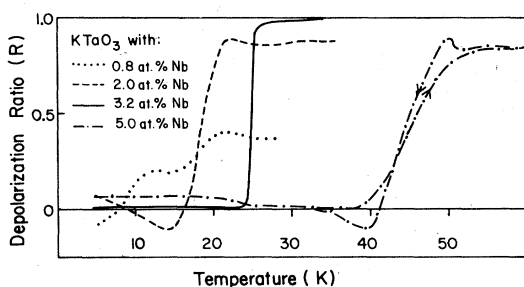


FIG. 3. Depolarization ratio of light ($\lambda = 514.5$ nm) after passing through KTN containing various Nb concentrations, measured as a function of temperature.

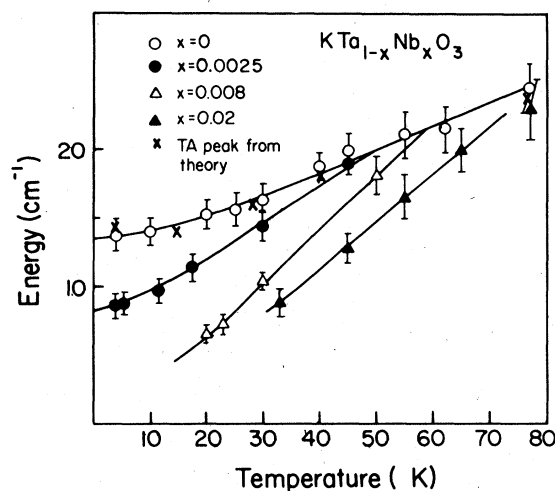


FIG. 4. Energy of the low-frequency scattering peak vs temperature for KTN containing several Nb concentrations. The points labeled x are calculated for a pure sample from the TA scattering model of Sec. IV. The lines are drawn as a guide to the eye. For $x = 0.008$, $T_c \approx 17$ K and for $x = 0.02$, $T_c \approx 28$ K.

scattering from the TO_1 branch, the Nb impurity is not a major contributor to the mechanism which breaks the lattice symmetry.

The question then arises: Are there any other features which vary with Nb concentration and which could conceivably provide information regarding the effect of Nb impurities on the lattice? A comparison of the Raman spectra for three Nb concentrations at 77 K, as shown in Fig. 5, indicates that there are two

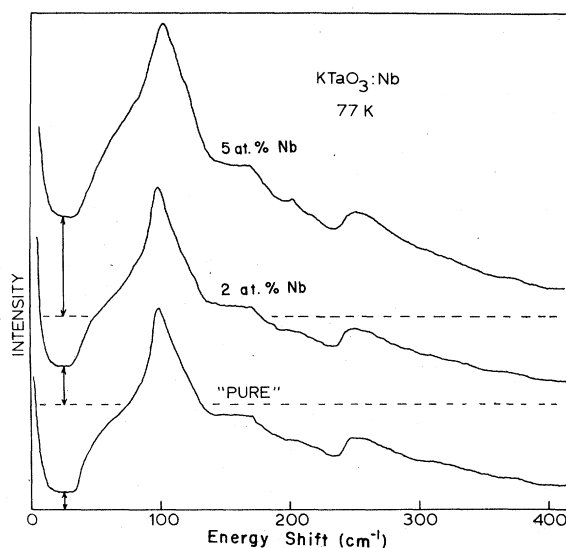


FIG. 5. Raman spectra of KTaO_3 with 0.0, 2, and 5 at. % Nb at 77 K. The dashed lines show the baseline in each trace.

possibilities for impurity-induced features. First, as indicated by the arrows at low energy, there is a very broad background that appears to increase with increasing niobium concentration at constant temperature. This background persists at temperatures far above the transition temperature. In order to determine whether this background is proportional to Nb concentration, the spectra obtained for a pure KTaO_3 sample at various temperatures were subtracted from the spectra of samples containing various Nb concentrations at the same temperatures. A comparison of such "subtracted" data for the 2 and 5 at. % Nb samples at nearly equal reduced temperatures, $[(T/T_c) - 1] \approx 1.5$, is shown in Fig. 6. There are three main components in each of these traces. First, the TO disorder-induced shoulder appears near 50 cm^{-1} because it shifts with Nb concentration and increases in intensity near T_c . Second, a sharp dip or derivative shape due to the broadened or shifted 2TA peak appears near 90 cm^{-1} . The third feature is the background, which is more clearly defined in the subtracted spectra, and is approximated by the dashed lines. This background is clearly larger for the 5 at. % Nb sample, and the difference would be even greater if the comparison were made at identical temperatures above the phase transition. Although there is some uncertainty regarding the effects due to the proximity to the differing transition temperatures in samples with varying Nb concentrations, it is possible that this background is due to some type of excitation involving the Nb ions.

The second possibility for a Nb-related feature in

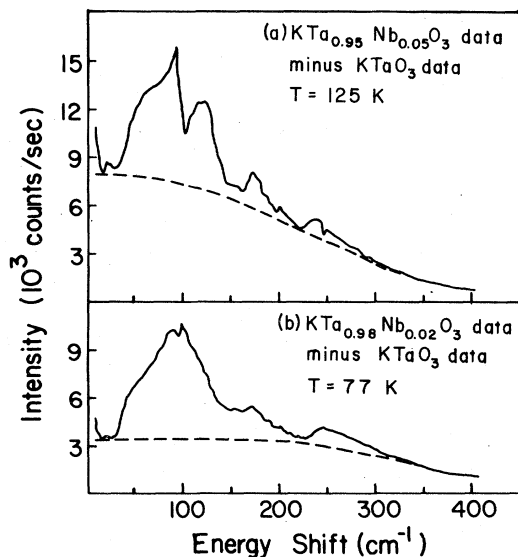


FIG. 6. Result of subtracting the Raman scattering data taken with a pure KTaO_3 sample from data taken with samples containing (a) 5 at. % Nb at 125 K and (b) 2 at. % Nb at 77 K.

the upper trace of Fig. 5 is a very weak, sharp peak near 200 cm^{-1} , which corresponds to first-order scattering from the zone-center TO_2 branch. This line is allowed in the ferroelectric phase and seems to persist, although with rapidly diminishing intensity, as the temperature increases above T_c , until it approaches a nearly constant value for $T \gg T_c$. Yacoby²⁹ has argued that this feature is evidence for fluctuations induced by the Nb defects. His analysis is based on the assumption that each Nb independently polarizes a large number (>10) of unit cells. This seems unlikely in view of the Nb concentration of 6 mole % used in Yacoby's work. Furthermore, the data presented here for samples with different Nb concentrations show no evidence of a correlation between the Nb concentration and the intensity of the TO_2 scattering. In view of the gradual changes in depolarization observed for most of these samples near the ferroelectric transition temperature, it seems most likely that the gradual disappearance of the TO_2 scattering is related to a distribution of transition temperatures in various regions of the sample. It is, therefore, primarily a property of the ferroelectric phase and not the paraelectric phase. Yacoby²⁹ rejects this possibility on the grounds that the TO_2 feature persists up to much higher temperatures than would be expected for such a mechanism. For the present samples, however, it was found that the residual TO_2 intensity observed far above T_c was not connected with the Nb concentration, but was essentially constant in all of the crystals, including those which were nominally pure. It is likely that this effect is a result of the same disorder mechanism that produces the first-order scattering from the TA and TO branches discussed in Sec. IV. If the constant background is added to the TO_2 intensity calculated for an assumed distribution of T_c , the discrepancies in Fig. 5 of Ref. 29 can be accounted for.

C. Electric-field-induced scattering

Softening of the low-frequency features of the Raman spectrum as the temperature approaches T_c could be an indication that the transition induced by Nb impurities is a classic soft-mode phase transition, in contrast to the transition observed in $\text{KTaO}_3:\text{Li}$ samples.³¹ In order to examine the validity of this hypothesis and to attempt to understand the low-frequency features in the Raman spectra of pure KTaO_3 , electric-field-induced Raman scattering experiments were undertaken. The electric-field-induced component of the Raman scattering in a 0.8 at. % Nb sample above the phase transition is shown in Fig. 7(a). For purposes of comparison, the input to the lock-in amplifier with zero applied electric field is shown on the same scale in Fig. 7(c). This comparison represents the best evidence that the shoulder corresponds to impurity-induced first-order scatter-

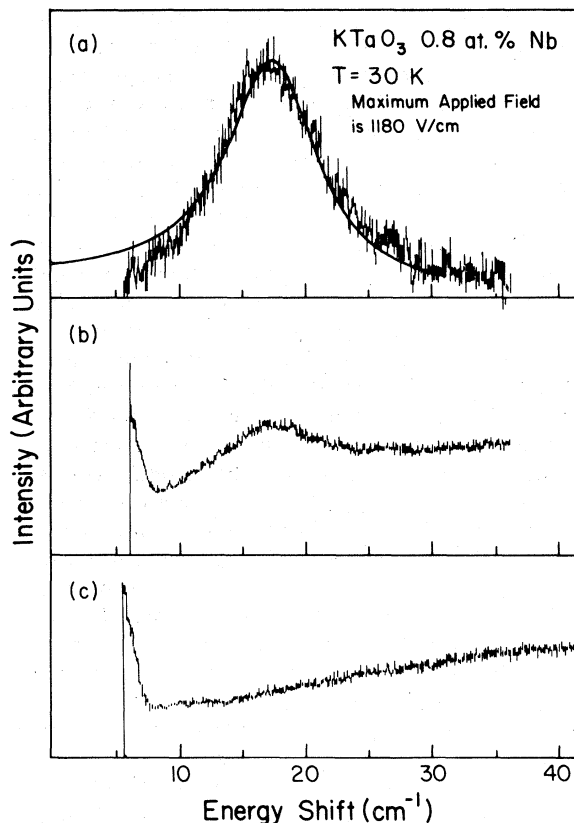


FIG. 7. (a) Electric-field-induced Raman scattering of KTaO_3 : 0.8 at.% Nb; (b) complete Raman spectrum taken simultaneously with (a); and (c) Raman spectrum under same conditions as (b) with no applied electric field.

ing from the soft mode.

The solid line in Fig. 7(a) represents the fit of a Lorentzian to the data, with a frequency ω_0 of 18.5 cm^{-1} and a width Γ of 8.8 cm^{-1} . The values of ω_0 which best fit the data at each temperature are given in Fig. 8. The observed soft-mode widths are essentially independent of temperature. These data were taken for the smallest amplitude of the electric field which would produce a reasonable signal-to-noise ratio (S/N) at each temperature. At 18 K, the maximum applied electric field was 300 V/cm, which is far less than the value of 1000 V/cm at which Fleury and Worlock failed to observe a change in the mode frequency due to the applied electric field. When the maximum applied field at 18 K was reduced by a factor of 2, the signal-to-noise ratio decreased, but changes in either the frequency or line shape were not observed. As the temperature was increased above T_c , the S/N ratio decreased even when the maximum applied field was increased to 2500 V/cm at 50 K. The width of the lines which fit the data changed from 8 cm^{-1} at 18 K to 10 cm^{-1} at 50 K with an uncertainty of 1 or 2 cm^{-1} . One interesting

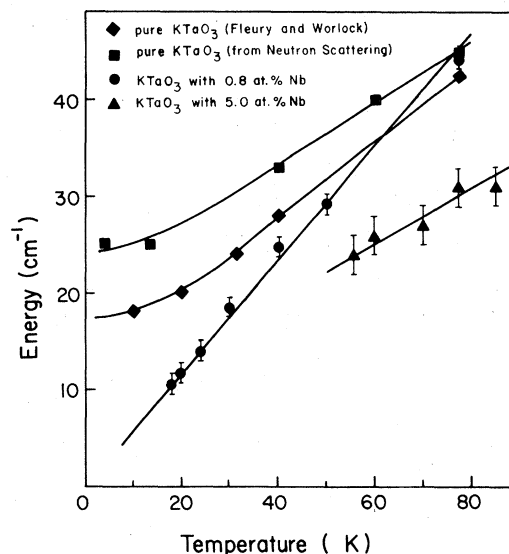


FIG. 8. Energy of the soft mode vs temperature determined from electric-field-induced scattering data. The lines are drawn as a guide to the eye.

feature of these data is that, while the lowest TO mode softened considerably and behaved very much like the mode driving the ferroelectric phase transition, the energy of the soft mode did not completely go to zero, nor did the mode become overdamped just above the phase transition. The soft mode retained an energy of about 10 cm^{-1} at 18 K, but its frequency did extrapolate to zero at about 0 K. This is consistent with the previous measurements of 0.8 at.% Nb as the critical Nb concentration for a ferroelectric phase transition at 0 K.³² Since the curve of T_c as a function of Nb concentration has infinite slope at this critical concentration, it is likely that inhomogeneities in the local Nb concentration will give rise to a large spread in T_c for different regions of the sample. In this case, features characteristic of the ferroelectric phase transition appear at about 17 K. Similar behavior is found for the elastic and dielectric properties of a sample from the same growth run.^{10,11}

Data were also taken for a KTaO_3 sample containing 5 at.% Nb at temperatures varying from 55 to 85 K. The values of ω_0 which best fit the data are plotted in Fig. 8. The primary difference between these data and the data obtained for the 0.8 at.% Nb sample is that, in the 5 at.% Nb sample, the soft mode stops softening at about 24 cm^{-1} at the phase transition. Furthermore, in the 5 at.% Nb sample, the linewidth of the soft mode increases as the transition is approached from above (from 22 cm^{-1} at 85 K to 36 cm^{-1} at 60 K). These effects are not currently understood, but it is possible that the differences in the data from the two samples are due either to cooperative effects between impurities in the 5 at.% Nb sam-

ple, or to a smearing of the phase transition in this sample, which is evident in Fig. 3.

IV. DISCUSSION

Evidence obtained in the present experiments suggests that the primary effect produced by adding low concentrations of Nb to KTaO_3 is a gradual reduction of the lowest zone-center TO frequency until the ferroelectric phase is stabilized at a given temperature. The fact that the Nb does not contribute to the disorder leading to the *A* and *B* features shown in Fig. 1 or to the TO_2 scattering suggests that this impurity is not in the categories of either "frozen" or "slowly relaxing" defects as discussed by Halperin and Varma.³³ Rather, it appears to conform to their classification *B3*, described as an impurity in a symmetric site which favors the low-temperature phase only "weakly" in the sense that any local departures from the symmetric phase occur on a time scale of the order of the TO phonon period. There is still the possibility of an odd-parity Nb resonance mode. Such a mode would be unobservable in an ordinary Raman scattering experiment and might be too weak or too broad to appear in the electric-field-induced scattering. The only possible evidence for such a mode might be the unexplained increase in the TO mode linewidth in the 5 at. % Nb sample near T_c and the broad background observed above T_c .

The observed decrease of the soft-mode frequency and stabilization of the ferroelectric phase with increasing Nb concentration occur despite the nearly identical size and much smaller mass of Nb^{5+} as compared with Ta^{5+} ($M_{\text{Nb}} \approx 0.5M_{\text{Ta}}$). These effects are probably attributable to a larger polarizability of the oxygen ion neighbors of the Nb. This increased polarizability will cause an increase in the long-range electric fields associated with the soft-mode displacements. Migoni *et al.*³⁴ have emphasized the importance of oxygen polarizability in stabilizing the ferroelectric phase in oxide crystals, and the large $T_c \approx 700$ K found⁹ for KNbO_3 is evidence of a much larger polarizability of the Nb-O coordination as compared with that of the Ta-O system.

The behavior of the soft-mode frequency in $\text{KTa}_{1-x}\text{Nb}_x\text{O}_3$ at the critical concentration $x_c = 0.008$ is of interest in connection with recent theoretical results³⁵⁻³⁷ for phase transitions in the "quantum limit" where $T_c \approx 0$.

Zero-point fluctuations modify the critical behavior of measurable quantities such as the dependences on x and T of T_c , the spontaneous polarization for $T < T_c$, and the susceptibility for $T > T_c$. In particular, the susceptibility has the form

$$\epsilon - \epsilon_\infty \propto (T - T_c)^{-\gamma}$$

for $T > T_c$, with $\gamma = 2$ in contrast to the classical

mean-field result, $\gamma = 1$. If the temperature dependences of all modes but the TO_1 mode are neglected, then the Lyddane-Sachs-Teller relation,

$$\frac{\epsilon(0)}{\epsilon(\infty)} = \frac{\omega_{\text{LO}}^2}{\omega_{\text{TO}}^2}$$

leads to the form of ω_{TO} given by

$$\omega_{\text{TO}} \propto (T - T_c)$$

In fact, the data in Fig. 8 do show a linear variation of ω_{TO} down to 17 K for the $x = 0.008$ sample. In view of the broadening of the phase transition in this sample, which prevented either measuring ω_{TO} at lower temperatures or obtaining an exact verification that $T_c = 0$, this result is not regarded as a definitive test of the quantum-limit critical exponents. Höchli *et al.*^{10,11} have examined this same series of samples. They found that the dependence on x of the spontaneous polarization P_s , the dielectric constant at $T = 0$ K, and the transition temperature T_c , as well as the dependence on temperature of $\epsilon(0) - \epsilon(\infty)$ for $x = 0.008$, were all consistent with the nonclassical critical exponents appropriate to the quantum limit. Thus, a variety of experiments, including the present Raman results, support the validity of this model in describing the low-temperature properties of $\text{KTaO}_3:\text{Nb}$.

The present studies also provide an increased understanding of the nature of the Raman spectrum observed for pure KTaO_3 . As noted in the previous section, a narrow peak is found at the energy of the second transverse-optic phonon at the zone center, even in the purest KTaO_3 samples. This peak must be the result of disorder in the lattice that breaks the translational symmetry leading to the wave-vector selection rule. The question that arises is then: If disorder-induced scattering is observed from the TO_2 mode, why is induced scattering from the lowest TO mode not observed. As has been shown, the shoulder *B* illustrated in Fig. 1 could easily be the result of such scattering. This explanation exacerbates the problem of accounting for the peak found below the shoulder. The peak appears to be related to the same disorder mechanism that induces scattering from both the TO_2 mode and the shoulder. In fact, *all three* of these features are enhanced by the addition of small concentrations of Li or Na in otherwise pure KTaO_3 .³¹ It has been suggested that the low-energy peak found below the shoulder is due to resonance modes of Li and Na impurities.³⁸ A more likely possibility, proposed here, involves disorder-induced scattering from the coupled TA and TO branches.

Axe *et al.*¹⁷ have found that the TA branch along $[00\xi]$ is strongly coupled to the soft TO branch, even in the harmonic approximation, and, as a result, the TA dispersion curve is modified to give a flat region near $\xi = 0.1$. They have fitted this behavior using a two-mode coupling theory in which the secular deter-

minant with respect to the $k = 0$ eigenvectors is given by

$$\begin{vmatrix} \omega_0^2 + f_{11} - \omega^2 & f_{12} \\ f_{12} & f_{22} - \omega^2 \end{vmatrix} = 0, \quad (1)$$

where ω_0 is the zone center TO branch frequency. In Eq. (1), the f_{ij} are approximated by the expansions

$$\begin{aligned} f_{11} &= (4.67 \times 10^3) \xi^2 - (2.4 \times 10^4) \xi^4, \\ f_{22} &= (1.83 \times 10^3) \xi^2 - (0.8 \times 10^4) \xi^4, \\ f_{12} &= (2.80 \times 10^3) \xi^2 - (2.4 \times 10^4) \xi^4, \end{aligned} \quad (2)$$

where f_{11} , f_{22} , and f_{12} are in units of meV^2 . These values give a reasonably good fit to the TA and TO dispersion curves measured along $[00\xi]$.

To illustrate the effects of this type of coupling on the disorder-induced scattering, the following approximations are made:

(i) The disorder is localized in the sense that only the displacements of atoms in at most a few unit cells are responsible for the scattering. The assumption can then be made that the scattered intensity for the TO branch is independent of wave vector and is proportional to the phonon-mode density out to values of $\xi \approx 0.2$.

(ii) The scattered intensity for the TA branch results solely from the admixed TO_1 eigenvector. This approximation is reasonable since the usual induced scattering from the TA branch is determined by the strain field of the TA phonon and would be negligible for $q \approx 0.1a^*$. The TO_1 eigenvector, however, is strongly admixed into the coupled TA branch and has large relative displacements of the atoms in a unit cell.

(iii) A one-dimensional dispersion is assumed for the TA branch, i.e., along $[00\xi]$. This amounts to neglecting the scattering contributions from regions of the dispersion curve for which q_x and q_y are nonzero. This approximation is justified to a considerable extent by assumption (ii) and by the rapid decrease of f_{12} for values of \bar{q} away from $[00\xi]$ observed in neutron scattering data. This can be seen in Fig. 2 of Ref. 15.

(iv) Since assumption (iii) is not valid for the TO_1 branch (an elliptical dispersion surface would be necessary), an attempt was not made to fit the TO_1 component of the scattering which produces the shoulder labeled *B* in Fig. 1.

From Eq. (1), the TA mode frequency is determined to be

$$\begin{aligned} 2\omega_{\text{TA}}^2(\xi) &= \omega_0^2 + f_{11} + f_{22} \\ &\quad - \{(\omega_0 + f_{11} + f_{22})^2 \\ &\quad + 4[f_{22}(\omega_0^2 + f_{11}) - f_{12}^2]\}^{1/2}. \end{aligned} \quad (3)$$

The eigenvector of the TA branch can be obtained

from the coupled mode equations

$$U_{\text{TA}}^i = A_1 U_{\text{TO}} + A_2 U_{\text{TA}},$$

where U_{TA} and U_{TO} are the uncoupled TA and TO_1 eigenvectors at $\xi = 0$ and

$$\begin{aligned} A_1 &= (1 - A_2^2)^{1/2} \\ &= f_{12} / [(\omega_0^2 - \omega_{\text{TA}}^2 + f_{11}) + f_{12}]^{1/2}. \end{aligned} \quad (4)$$

Using Eqs. (2), (3), and (4), the scattered TA intensity can be obtained from

$$I_{\text{TA}}(\omega) = c \int_0^{0.5} A_1^2(\xi) \frac{d\omega_{\text{TA}}}{d\xi} \delta(\omega - \omega_{\text{TA}}) d\xi, \quad (5)$$

where c is a constant.

The calculated distribution, allowing for experimental resolution, is shown as closed circles in Fig. 1. Values of ω_0 used in these calculations were obtained from the neutron scattering results of Shirane *et al.*,¹⁶ and the f_{ij} in Eqs. (2) were assumed to be independent of temperature, so that only c is adjusted in order to scale the intensity distribution. The position of this calculated peak as a function of temperature is shown by crosses in Fig. 4. The agreement between the calculated and measured positions is reasonable, but the width of the calculated peak is substantially narrower than the observed one. Attempts were made to improve this fit by adding a frequency-independent damping to the TA branch, but the exact shape of the peak could not be accounted for. Other possible reasons for this discrepancy in peak width include the effects of three-dimensional TA dispersion, frequency-dependent damping, anharmonicity, or simply the inaccuracy of the f_{ij} obtained from the neutron scattering data (see, for example, Fig. 4 of Ref. 17). In view of these uncertainties, any further refinement of the calculation was judged to be unwarranted.

Despite the lack of complete correspondence in fitting the experimental spectra, the above explanation of the low-frequency scattering peak *A* is consistent with a number of its properties: its intensity is comparable to that of the TO-induced scattering, and it has the same polarization characteristics; its shift with temperature and Nb concentration are correctly predicted on the basis of the corresponding TO_1 mode shifts; its intensity increases when strongly symmetry-breaking defects such as off-center Li and Na are present. The remaining question, therefore, concerns the origin of the disorder-induced scattering observed for nominally pure KTaO_3 . It is possible that this scattering is due either to intrinsic disorder in the crystals or to impurities such as Li, Na, or OH^- that might be present in the original starting materials or could be introduced during the crystal growth process. Of these impurities, OH^- is known to be present³⁹ in most "as-grown" samples at con-

centrations up to 10^{18} cm^{-3} . Recent evidence indicates that if OH^- impurities are not present, the intensity of the TA scattering peak is considerably reduced, but the TO_1 branch scattering is not noticeably affected. Thus, there may be even more than one type of disorder mechanism. It is of interest to note that other evidence for large-scale disorder in the paraelectric phases of KTaO_3 and other oxide perovskites has been found from neutron and Raman scattering studies. For example, a strong, quasielastic, $\bar{q} \approx 0$ neutron scattering background has been observed in both KTaO_3 (Ref. 17) and orthorhombic KNbO_3 .⁴⁰ Like the disorder-induced scattering observed in the present series of investigations, this anomalous scattering is found at temperatures far removed from T_c and its intensity is relatively insensitive to temperature. It has been suggested⁴¹ that this disorder results from an intrinsic disorder mechanism involving linear chains of static or dynamic ferroelectric ordering along $\langle 100 \rangle$ directions. In fact, the polarization character of the disorder-induced Raman scattering observed here for the TA and TO branches is consistent with a disorder mechanism of this type, which would produce a distortion of the same symmetry, T_{1u} , as the $\bar{q} \approx 0$ TO branch. The TO phonon polarized along such a linear chain would transform as a totally symmetric vibration in the reduced symmetry and would therefore appear only in diagonal polarization geometries.

V. SUMMARY

A number of conclusions have been reached based on the measurements described here. First, the introduction of over 0.8 at. % of Nb impurities into KTaO_3 induces a ferroelectric phase with a transition temperature which increases monotonically with increasing Nb concentration. While there are changes in the Raman spectrum that are related to the pres-

ence of the phase transition, there are no sharp features with energies greater than 3 cm^{-1} which can be related to the Nb concentration in a definitive manner. However, a broad background of scattered light in the paraelectric phase appears to be connected in some way with the presence of Nb.

For any Nb concentration that induces the ferroelectric phase transition, the energy of the lowest zone-center TO phonon is found to decrease with decreasing temperature, but the energy fails to exactly reach zero at T_c . As the temperature is decreased below T_c , the Raman-active TO phonon energy is observed to increase from a low, but nonzero value near T_c . Thus, while the phase transition behaves very much like a simple soft-mode transition at temperatures far from T_c , there is a temperature range that is larger than the traditional critical region in which the dynamic behavior of the system is more complex.

Since the soft zone-center TO mode decreases in frequency at a given temperature as the Nb concentration increases, the behavior of KTaO_3 is like that of a one-mode mixed crystal system as far as the TO branch energy region is concerned, and Nb shows no evidence of being a symmetry-breaking defect.

Disorder-induced scattering is observed from the coupled TA and TO branches. It is believed that this mechanism accounts for the temperature-dependent low-frequency features which have been attributed in the past to an impurity resonance mode and to two-phonon scattering.

ACKNOWLEDGMENTS

This work was supported in part by NSF Grant No. DMR 78-09426. The Oak Ridge National Laboratory is operated by Union Carbide Corporation for the U.S. Department of Energy under Contract No. W-7405-eng-26.

- ¹U. T. Höchli and L. A. Boatner, *J. Phys. C* **10**, 4319 (1977).
- ²S. H. Wemple, *Phys. Rev.* **137**, A1575 (1965).
- ³G. Rupprecht and R. O. Bell, *Phys. Rev.* **135**, A748 (1964).
- ⁴R. P. Lowndes and A. Rastagi, *J. Phys. C* **6**, 932 (1973).
- ⁵W. R. Abel, *Phys. Rev. B* **4**, 2696 (1971).
- ⁶G. A. Samara and B. Morosin, *Phys. Rev. B* **8**, 1256 (1973).
- ⁷H. Uwe and T. Sakudo, *J. Phys. Soc. Jpn.* **38**, 183 (1975).
- ⁸H. Uwe, H. Unoki, Y. Fujii, and T. Sakudo, *Solid State Commun.* **13**, 737 (1973).
- ⁹S. Triebwasser, *Phys. Rev.* **114**, 63 (1959).
- ¹⁰U. T. Höchli, H. Weibel, and L. A. Boatner, *Phys. Rev. Lett.* **39**, 1158 (1977).
- ¹¹U. T. Höchli and L. A. Boatner, *Phys. Rev. B* **20**, 266 (1979).
- ¹²D. Rytz, L. A. Boatner, A. Châtelain, U. T. Höchli, and K.

- A. Müller, *Helv. Phys. Acta* **51**, 430 (1978).
- ¹³W. B. Yelon, W. Chochran, G. Shirane, and A. Linz, *Ferroelectrics* **2**, 261 (1971).
- ¹⁴A. W. Hewatt, K. D. Rouse, and G. Zaccai, *Ferroelectrics* **4**, 153 (1972).
- ¹⁵G. Zaccai and A. W. Hewatt, *J. Phys. C* **7**, 15 (1974).
- ¹⁶G. Shirane, R. Nathans, and V. J. Minkiewicz, *Phys. Rev.* **157**, 396 (1967).
- ¹⁷J. D. Axe, J. Harada, and G. Shirane, *Phys. Rev. B* **1**, 1227 (1970).
- ¹⁸R. Comés and G. Shirane, *Phys. Rev. B* **5**, 1886 (1972).
- ¹⁹R. C. Miller and W. G. Spitzer, *Phys. Rev.* **129**, 94 (1963).
- ²⁰C. H. Perry and T. F. McNelly, *Phys. Rev.* **154**, 456 (1967).

- ²¹W. G. Nilsen and J. G. Skinner, *J. Chem. Phys.* 47, 1413 (1967).
- ²²C. H. Perry, J. H. Fertel, and T. F. McNelly, *J. Chem. Phys.* 47, 1619 (1967).
- ²³P. A. Fleury and J. M. Worlock, *Phys. Rev. Lett.* 18, 665 (1967).
- ²⁴P. A. Fleury and J. M. Worlock, *Phys. Rev.* 174, 613 (1968).
- ²⁵Y. Yacoby and A. Linz, *Phys. Rev. B* 9, 2723 (1974).
- ²⁶S. K. Manlief and H. Y. Fan, *Phys. Rev. B* 5, 4046 (1972).
- ²⁷Y. Yacoby, F. Cedeira, M. Schmidt, and W. B. Holzapfel, *Solid State Commun.* 14, 1325 (1974).
- ²⁸H. Uwe and T. Sakudo, *Phys. Rev. B* 15, 337 (1977).
- ²⁹Y. Yacoby, *Z. Phys. B* 31, 275 (1978).
- ³⁰L. A. Boatner, A. H. Kayal, and U. T. Höchli, *Helv. Phys. Acta* 50, 167 (1977).
- ³¹R. L. Prater, L. L. Chase, and L. A. Boatner (unpublished).
- ³²L. A. Boatner, U. T. Höchli, and H. Weibel, *Helv. Phys. Acta* 50, 620 (1977).
- ³³B. I. Halperin and C. M. Varma, *Phys. Rev. B* 14, 4030 (1976).
- ³⁴R. Migoni, H. Bilz, and D. Baurle, *Phys. Rev. Lett.* 37, 1155 (1976).
- ³⁵R. Oppermann and H. Thomas, *Z. Phys. B* 22, 337 (1975).
- ³⁶T. Schneider, H. Beck, and E. Stoll, *Phys. Rev. B* 13, 1123 (1976).
- ³⁷R. Morf, T. Schneider, and E. Stoll, *Phys. Rev. B* 16, 462 (1977).
- ³⁸Y. Yacoby, *Z. Phys. B* 24, 397 (1976).
- ³⁹Herbert Engstrom, J. B. Bates, and L. A. Boatner, *J. Chem. Phys.* 73, 1073 (1980).
- ⁴⁰R. Currat, R. Comés, B. Dorner, and E. Wiesendanger, *J. Phys. C* 7, 2521 (1974).
- ⁴¹M. Lambert and R. Comés, *Solid State Commun.* 7, 305 (1969); R. Comés, M. Lambert, and A. Guinier, *J. Phys. Soc. Jpn.* 28, 195 (1970).